10-30-2019

Condensed Phase Deactivation of Solid Brønsted Acids in the Dehydration of Fructose to Hydroxymethylfurfural

Robert L. Johnson
Iowa State University and University of Hawaii at Manoa

Frédéric A. Perras
Ames Laboratory, fperras@ameslab.gov

Michael P. Hanrahan
Iowa State University and Ames Laboratory, mph@iastate.edu

Max A. Mellmer
University of Wisconsin

Thomas Garrison
King Fahd University of Petroleum & Minerals

See next page for additional authors

Condensed Phase Deactivation of Solid Brønsted Acids in the Dehydration of Fructose to Hydroxymethylfurfural

Abstract

Catalyst deactivation resulting from the hydrothermal leaching of sulfonic acid residues and the deposition of carbonaceous residues were studied using condensed phase flow reactor experiments along with state-of-the-art solid-state NMR. Several commercially available sulfonic acid-containing heterogeneous Brønsted acids were compared by measuring the rates of sulfonic acid breakdown at hydrothermal flow conditions of 160 oC. Amberlyst 45 was found to show higher hydrothermal stability when compared to both Nafion and Amberlyst 15, with <10% loss in acidity after 48 h. The dehydration reaction of fructose to hydroxymethylfurfural (HMF) was used as a model system to compare deactivation rates from carbon deposition (fouling) to those from sulfur leaching, and deactivation from fouling was shown to be dramatically faster than that from sulfonic acid leaching alone. Fouling rates were then investigated in greater detail by comparing the influence of several factors including reactant, solvent, residence time, and feed concentration. The only successful approach to minimize fouling was the use of a polar aprotic solvent (DMSO) with dilute (50 mM) reactant streams. In aqueous systems operating the reactor in a regime with low conversion conditions (short residence times) does not significantly improve the longevity of the catalyst. Spent catalysts were characterized using 13C solid-state NMR spectroscopy enhanced by dynamic nuclear polarization (DNP). Additionally, in situ 1H and 13C high-resolution magic angle spinning (HR-MAS) solid-state NMR spectroscopy was used to investigate the solvent influence at the catalyst interface. The HR-MAS NMR studies showed that in polar aprotic solvents, the increased acidity leads to greater selectivity towards HMF; more importantly, that the dehydration products do not readily adhere to the surface in DMSO, in contrast to their behavior in water. The results demonstrate that more active and longer-lived acid catalysts could be obtained by tuning the solvent and surface polarity to allow for efficient desorption of products, thereby reducing the catalyst deactivation that occurs due to fouling.

Keywords

Fructose dehydration, Solid acid catalysis, Stability, Catalyst characterization, DNP SSNMR

Disciplines

Chemistry

Authors

Robert L. Johnson, Frédéric A. Perras, Michael P. Hanrahan, Max A. Mellmer, Thomas Garrison, Takeshi Kobayashi, James A. Dumesic, Marek Pruski, Aaron Rossini, and Brent H. Shanks

Condensed Phase Deactivation of Solid Brønsted Acids in the Dehydration of Fructose to Hydroxymethylfurfural

Robert L. Johnson[a,e,g], Frédéric A. Perras[,d], Michael P. Hanrahan[b,d], Max Mellmer[f], Thomas F. Garrison[c], Takeshi Kobayashi[d], James Dumesic[a,f], Marek Pruski[b,d], Aaron J. Rossini[b,d], Brent H. Shanks[a,e]*

[a]Chemical and Biological Engineering Department Iowa State University, Ames, IA 50011 USA

[b] Department of Chemistry, Iowa State University, Ames, IA 50011 USA

[c] Department of Chemistry, King Fahd University of Petroleum & Minerals, Dhahran 31261, Saudi Arabia.

[d] US DOE, Ames Laboratory, Ames IA 50011-3020 USA

[e] Center for Biorenewable Chemicals (CBiRC), Ames, IA 50011 USA

[f] Department of Chemical and Biological Engineering University of Wisconsin, Madison, WI 53706 USA

[g] Hawaii Natural Energy Institute, University of Hawaii at Manoa, Honolulu, HI 96822 USA

ABSTRACT: Catalyst deactivation resulting from the hydrothermal leaching of sulfonic acid residues and the deposition of carbonaceous residues were studied using condensed phase flow reactor experiments along with state-of-the-art solid-state NMR. Several commercially available sulfonic acid-containing heterogeneous Brønsted acids were compared by measuring the rates of sulfonic acid breakdown at hydrothermal flow conditions of 160 °C. Amberlyst 45 was found to show higher hydrothermal stability when compared to both Nafion and Amberlyst 15, with <10% loss in acidity after 48 h. The dehydration reaction of fructose to hydroxymethylfurfural (HMF) was used as a model system to compare deactivation rates from carbon deposition (fouling) to those from sulfur leaching, and deactivation from fouling was shown to be dramatically faster than that from sulfonic acid leaching alone. Fouling rates were then investigated in greater detail by comparing the influence of several factors including reactant, solvent, residence time, and feed concentration. The only successful approach to minimize fouling was the use of a polar aprotic solvent (DMSO) with dilute (50 mM) reactant streams. In aqueous systems operating the reactor in a regime with low conversion conditions (short residence times) does not significantly improve the longevity of the catalyst. Spent catalysts were characterized using ^{13}C solid-state NMR spectroscopy enhanced by dynamic nuclear polarization (DNP). Additionally, in situ ^{1}H and ^{13}C high-resolution magic angle spinning (HR-MAS) solid-state NMR spectroscopy was used to investigate the solvent influence at the catalyst interface. The HR-MAS NMR studies showed that in polar aprotic solvents, the increased acidity leads to greater selectivity towards HMF; more importantly, that the dehydration products do not readily adhere to the surface in DMSO, in contrast to their behavior in water. The results demonstrate that more active and longer-lived acid catalysts could be obtained by tuning the solvent and surface polarity to allow for efficient desorption of products, thereby reducing the catalyst deactivation that occurs due to fouling.

Keywords:

Fructose dehydration, Solid acid catalysis, Stability, Catalyst characterization, DNP SSNMR

1. INTRODUCTION

The substitution of bio-based chemicals and fuels for those derived from petroleum feedstocks has attracted renewed interest in the last decade.[1-6] One of the promising platforms for these efforts is the conversion of carbohydrates into furanic molecules, which can then be used to produce a large number of molecules analogous to those derived from petroleum.[7-9] Isomerization of glucose to fructose followed by Brønsted acid-catalyzed dehydration leads to hydroxymethylfurfural (HMF). HMF obtained from biomass can then be used to produce a variety of industrially relevant products.[10] Unlike with petroleum, the series of reactions for converting carbohydrates into HMF requires condensed phase processing conditions. To date, batch reactions in polar aprotic solvents, catalyzed with homogeneous acid, have been demonstrated as the most effective strategy for obtaining high yields of HMF from fructose.[11-13] Although this route is effective, improvement in the environmental footprint and processing cost may be possible through substitution of the homogeneous acid catalyst with a heterogeneous catalyst.

The replacement of homogeneous catalysts requires a heterogeneous acid catalyst that remains active in the relevant condensed phase reaction conditions (containing 5-100% H_2O) at elevated temperatures (ranging from 100-200 °C). The issue of acid catalyst stability under hydrothermal conditions has been a central investigative theme for catalyst research in the area of biomass conversion.[14,15] Brønsted/Lewis acid catalysts, such as silica-alumina, γ-Al_2O_3,[16] and zeolites[17,18] are known to break down under hydrothermal conditions. Catalyst materials containing sulfonic acid active sites, including polymeric resins and sulfonated carbon materials, are also susceptible to breakdown under hydrothermal conditions, despite the carbon scaffold being hydrothermally stable. Under hydrothermal conditions, sulfonic acid groups are readily hydrolyzed, leading to leaching.[8,19,20] For example, common resins such as Amberlyst 15, sulfonated carbon materials, as well as porous silica with sulfonic acid groups grafted onto the silica surface, rapidly deactivate at hydrothermal conditions above 120 °C. Considering that the temperatures required for dehydration of fructose to HMF need to reach between 140 to 160 °C with the water content in the solvent system exceeding 30%, the vast majority of available sulfonated materials lack sufficiently stable sulfonic acid groups to be viable catalysts for converting fructose to HMF under realistic processing conditions.

Significant improvement in sulfonic acid hydrothermal stability has been reported for Amberlyst 45, a heavily cross-linked and halogenated sulfonated polystyrene resin having a stabilized macromolecular structure and strengthened sulfonic acid linkage.[21] Surprisingly, after treatment in batch conditions for 6 h at 180 °C, only a 9% reduction in acidity was observed.[21] An alternative class of materials to carbon and resins is sulfated zirconia.[22] Recently, a method to synthesize mesoporous sulfated zirconia was reported, wherein SBA-15 was used as a template for deposition of zirconium oxide monolayers. These materials were confirmed to have excellent catalytic properties with the silica effectively protected from hydrothermal breakdown.[22] Both of these reports, however, did not rigorously test the hydrothermal stability of these materials, since the reactions were carried out under batch conditions instead of flow reactor conditions, and the exposure times were limited. Furthermore, the evidence used to validate the hydrothermal stability of templated sulfated zirconia was based only on porosimetry and XRD measurements which does not provide a direct measurement of the number of active sites on the material.[22]

Previous research on catalyst stability for solid Brønsted acids in condensed phase applications has focused primarily on reducing the rate of active site leaching by improving the strength of the sulfonic acid linkage. However, it has not yet been clearly established that leaching of sulfur is the dominant mechanism of catalyst deactivation when using state-of-the-art solid Brønsted acid catalysts. For example, it is well known that for palladium-catalyzed condensed phase hydrogenation reactions, the catalyst deactivation from fouling is quite rapid compared to rates of sintering or metal leaching.[23] A better understanding of deactivation mechanisms in solid Brønsted acid catalysts is required in order to develop catalysts with improved stability.

To the best of our knowledge, no previous comparison of deactivation rates from fouling and leaching of sulfur has been performed for heterogeneous Brønsted acid catalysts under relevant processing conditions. To address this question, we performed a series of experiments to independently measure the rates of hydrothermal sulfur leaching and fouling. Moreover, we investigated the critical factors for reducing the rate of catalyst fouling. Lastly, ^{13}C NMR

experiments were performed on both fresh catalysts and deactivated catalyst materials to elucidate the mechanisms responsible for carbon deposition when reactions are run using water as the solvent.

2. MATERIALS AND METHODS

2.1 Reagents

All chemicals were purchased from Sigma-Aldrich (St. Louis, MO, USA) and used without additional purification. UHP+ quality gases (99.995%) for BET were purchased from Airgas (Radnor, PA, USA). Water was filtered using a Barnstead E-pure system and allowed to reach 18.1 MΩ resistance for all applications. U-^{13}C-enriched fructose (99.8%) and d_6-DMSO were purchased from Cambridge Isotope Laboratories (Tewksbury, MA, USA).

2.2 Materials synthesis

Synthesis of sulfated zirconia was carried out according to a previously reported method[24] using open pore Davisil silica. Materials were compressed into pellets and sieved to collect particles ranging from 450 to 600 µm. The pelletized materials were dried in a muffle furnace at 300 °C for 4 h and transferred to a glove box. Then, 2.2 g (total surface area of approximately 616 m^2) of silica was mixed with 6 g of zirconium (IV) propoxide (70 wt% in propanol) in 30 mL of anhydrous hexane and allowed to reflux at 70 °C overnight. The material was filtered, rinsed three times with hexane to remove any residual unreacted precursor, rehydrated with 30 mL of deionized water with stirring for 4 h, and finally dried at 80 °C overnight. Sulfation was carried out by soaking materials (1 g/30 ml) in 0.25 M H_2SO_4 at room temperature for 5 h. Samples were then filtered and dried at 80 °C overnight followed by calcination at 550 °C for 3 h.

2.3 Hydrothermal treatments of solid acids

Hydrothermal treatments were performed using a high-pressure flow reactor system capable of operation at pressures up to 80 bar and 400 °C. Material flow was regulated using a Brooks SLA 5850 mass flow controller for gases (Brooks Instruments, Hatfield, PA, USA) and a Series I HPLC pump for liquids (Scientific Systems, State College, PA, USA). The temperature was controlled using an Omega CSi32 series temperature controller with a K-type thermocouple (Omega Engineering, Norwalk, CT, USA). Temperature was maintained within ± 1°C during the treatments. (See SI for schematic and pictures.) A liquid flow rate of 0.02 mL/min was used. Liquids were removed and stored in a −4 °C freezer until analysis. Remaining solids were removed from the reactor bed and dried at 105 °C prior to final analysis.

2.4 Dehydration reactions

Samples were analyzed using a Waters Alliance HPLC system equipped with having a Phenomenex size exclusion column (65 °C) equipped with a Waters PDA/refractive index detector (Waters Corporation, Milford, MA, USA). Samples were eluted isocratically with a 5 mM sulfuric acid mobile phase at a flow rate of 0.7 mL/min.

2.5 Acid site quantification

The number of strong acid sites was determined via titration using a Titrino autotitrator (Metrohm AG, Herisau, CH). The titration mixtures were prepared by mixing approximately 200-500 mg of wet solid in 30 ml of a 1 M potassium chloride solution, which was then titrated with a 0.05 M sodium hydroxide solution at a dosing rate of 0.25 mL/min. Samples were degased prior to titration for 5 minutes by bubbling nitrogen with constant stirring. The number of acid sites was calculated based on the number of moles of sodium hydroxide required to reach the equivalence point, i.e., the inflection point in the titration curve, and was normalized on a dry mass basis.

2.6 DNP-enhanced ^{13}C solid-state NMR

DNP-enhanced solid-state NMR experiments were performed using a Bruker AVANCE III 400 MHz MAS-DNP NMR system (Bruker Corp, Billerica, MA, USA) equipped with a 3.2-mm low-temperature magic angle spinning (MAS) probe and a 9.7 T gyrotron. The 20 mg catalyst sample was impregnated with a 10 mM solution of the AMUPol polarizing agent[25] (Cortecnet, Voisins-le-Bretonneux, France) in H_2O and packed into a 3.2-mm sapphire rotor, which was then sealed with a Teflon plug. The sample temperature was approximately 110 K and the MAS frequency was set to 10 kHz. A 1D ^{13}C NMR spectrum was acquired using cross-polarization (CP) using a 2.75 µs ^{1}H excitation pulse and a 1.5 ms contact time. A total of 16k scans were accumulated with a 1 s recycle delay. A 2D 1H-^{13}C HETCOR spectrum was obtained with PRESTO-II (phase-shifting effects a smooth transfer of polarization)[26] for the ^{1}H→^{13}C coherence transfer step since it has been shown that PRESTO-II transfers yield only 1-bond correlations with improved sensitivity when compared with through-bond transfers.[27] Six pulse pairs of $R18^7_1$ heteronuclear recoupling were used for the transfer and a ^{13}C rf pulse magnetic field of 50 kHz was used for all the ^{13}C pulses. Frequency-switched Lee-Goldburg (FSLG)[28] ^{1}H homonuclear

decoupling was applied during t_1 to improve the ^{1}H resolution. Thirty-two t_1 increments of 48 µs, each consisting of 5120 scans, were acquired, and the States-TPPI method was used for phase-sensitive 2D acquisition.

2.7 Solid-State NMR Experiments on Impregnated Catalysts

Impregnated materials were prepared inside a glovebox for analysis with in situ NMR by weighing out approximately 10 mg of catalyst material into a 2-mL screw-cap polypropylene tube. Liquid was then applied to the solid material and allowed to equilibrate for a minimum of 6 h (typically overnight). Since the solid substrates were coated with 0.667 µL/mg catalyst and the average surface area for the solids was 300 m^2/g, this translated, on average, to an approximately 2-nm layer of catalyst deposited onto the samples. Following an equilibration period, samples were agitated using a spatula and then packed in the 2.5-mm MAS rotor in the glove box. Rotors were weighed before and after NMR experiments to ensure that no liquid was lost during the experiments. ^{1}H, ^{13}C and ^{29}Si NMR experiments were carried out on a Bruker Avance III HD 400 MHz solid-state NMR spectrometer (Bruker Corp, Billerica, MA, USA) equipped with a triple resonance 2.5-mm HXY probe. The ^{1}H solid-state NMR spectra were acquired using a spin echo sequence under static and 25 kHz MAS, with 100 kHz excitation and refocusing pulses, 8-16 scans, 2 s repetition delay and an echo delay of 40 µs. The ^{13}C solid-state NMR spectra were acquired using either Bloch decay or cross-polarization (CP) pulse sequences. The MAS frequency was 25 kHz and SPINAL-64 heteronuclear decoupling applied during acquisition with a 100 kHz ^{1}H rf field. For the Bloch decay spectra the ^{13}C excitation pulse with an rf field of 73.5 kHz was used with 32 to 512 scans and a recycle delay between 5-10 s. For the ^{1}H-^{13}C CPMAS NMR experiments the initial ^{1}H excitation had a 100 kHz rf field and the CP match condition used 77 kHz and 121 kHz rf field spin-lock pulses for ^{13}C and ^{1}H, respectively, with a 3 ms CP contact time. The ^{1}H spin lock pulses rf was linearly ramped from 85% to 100% of the rf field. CPMAS spectra were acquired with a 2 s recycle delay and 128 scans.

2D ^{1}H-^{1}H NOESY spectra were acquired on a Varian 600 MHz NMR System spectrometer equipped with a 1.6-mm triple-resonance MAS probe. The samples were packed into zirconia rotors and spun at 20 kHz. The spectra were obtained using a ^{1}H rf pulse magnetic field of 100 kHz, 800 t_1 points with an interval of 100 µs, 8 scans per t_1 point and the STATES-TPPI method for quadrature detection.

3. RESULTS AND DISCUSSION

3.1 Deactivation from sulfur leaching vs. carbon deposition

Our initial objective was to examine the relative rates of acid site loss due exclusively to hydrothermal leaching of sulfonic acid groups. To this end, several commercially available sulfonic acid-containing resins (Amberlyst 15, 45, and Nafion) were tested under hydrothermal flow conditions, using more rigorous criteria than repeated batch conditions. The changes in acid sites, determined by titration after the packed beds were subjected to a continuous stream of ultra-purified water heated to 160 °C and pressurized to 550 psi, are shown in Figure 1 (solid symbols). Nafion coated onto porous silica was quite labile under these conditions and showed no detectable strong acid groups after only 24 h on stream. This finding was not surprising considering the relatively weak O-ether linkage that binds the perfluorinated side group to the polymer backbone. Amberlyst 15, a typical sulfonated polystyrene resin, displayed far better stability than Nafion, although the acid sites on Amberlyst 15 still decomposed quite rapidly with an observed reduction from 4.8 mmol/g to 1.8 mmol/g in 24 h on stream. In addition to the loss of acid sites, the polymeric backbone was observed to decompose under these conditions, as evidenced by residue on the filter paper. However, Amberlyst 45 (previously known as Amberlyst 70)[21] only showed a minor loss (<10%) of acid sites after 48 h on stream; after 120 h only 25-33% was lost. Furthermore, in contrast to Amberlyst 15, the polymeric backbone integrity seemed to be maintained as no residues were observed following the filtration. The results under hydrothermal flow conditions confirmed previous reports of this material's high extent of hydrothermal stability. The demonstration of hydrothermal stability for time periods of days on stream was especially remarkable given the severity of these treatments.

To expand on the results demonstrating the relative time scales required for hydrothermal breakdown of Amberlyst 45 acid groups, a series of experiments were conducted under identical pressure/temperature/flow conditions with the addition of two different polyol reactants. From these experiments, a relative comparison of the deactivation rates from carbon deposition to that of sulfur leaching could be obtained. The two polyol reactants were fructose and 1,2,6-

hexanetriol, specifically selected because they provide a comparison between furan and pyran dehydration products and because they are relevant systems for condensed phase biomass conversion schemes.

The resulting loss of acidity for Amberlyst 45 was striking when a 1 M fructose solution was substituted for water, resulting in 90% reduction of acid sites after only 12 h on stream and 95% reduction after 24 h on stream. This corresponded to a 25-fold greater deactivation rate from fouling compared to hydrothermal leaching of sulfur. A similar, albeit weaker, trend was observed when 1.6 M 1,2,6-hexanetriol was used under the same flow and temperature conditions. Here, the fouling rate from 1,2,6-hexanetriol was less than that from fructose, corresponding to a deactivation rate that was only 5.6-fold greater than that due to sulfur leaching alone.

The difference in the fouling rates for fructose and 1,2,6-hexanetriol was not surprising considering that different reaction pathways lead to the formation of different classes of dehydration products, namely pyrans in the case of 1,2,6-hexanetriol and furans from fructose.[29] It is known that humin formation rapidly occurs when furanic compounds polymerize during exposure to hydrothermal conditions. Furthermore, the dehydration of fructose has a lower activation energy than that of 1,2,6-hexanetriol, since a more labile hydroxyl group is attached to the anomeric carbon. Importantly, these experiments showed that hydrothermal deactivation via fouling, when using the state-of-the-art sulfonated resins, occurred on the time scale of hours, as compared to days for the hydrothermal leaching of sulfur. These findings clearly implied that the main issue for hydrothermal stability is not the leaching of acid or decomposition of support material but the rate of fouling.

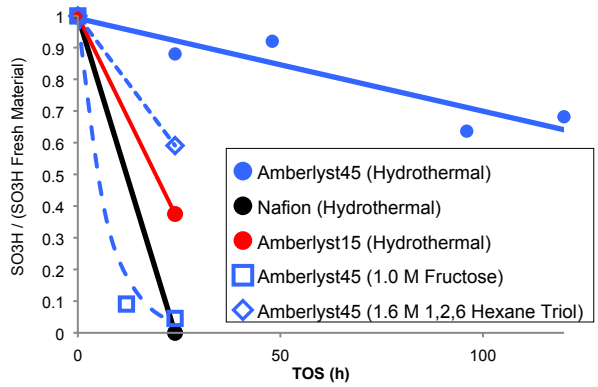

Figure 1. Change in the number of strong acid sites (as determined via titration) as a function of time on stream (TOS) in plug flow hydrothermal treatments at 160 °C with a flow rate of 0.02 ml/min.

3.2 Deactivation under reaction conditions

To determine other factors influencing deactivation, additional experiments were run in which changes in the conversion/selectivity of fructose towards HMF were measured under a variety of reaction conditions. These experiments were designed to elucidate what factors could be leveraged to reduce the rate of fouling. First, the reactor was run under conditions of low conversion to mitigate deactivation. Second, the influence of the solvent on the rate of fouling was compared by running a series of experiments using a polar aprotic solvent (DMSO) instead of water. Finally, the relationship between the initial feed concentration and rate of deactivation was determined.

3.2.1 Reactions in H_2O

Results comparing deactivation as a function of conversion, i.e., residence time (Figure 2A, filled circles), showed that the deactivation rate was lower when the reactor was run at lower conversion condition (0.175 h^{-1} at 40% initial conversion vs. 0.334 h^{-1} at 80% initial conversion). The deactivation rate at 80% conversion was 110 times greater than the rate of hydrothermal sulfur leaching, suggesting that the fouling rate determined in the previous experiment was limited by the molar flow rate of fructose. Notably, even when the reactor was run with low initial conversion (<50%), the rate of fouling was still 60 times greater than the hydrothermal leaching of sulfur, with the catalyst being deactivated in hours.

When the reactor was run at a high fructose conversion condition, the HMF selectivity was initially very low and then increased as the fructose conversion precipitously dropped. Conditions with lower fructose conversion lead to improved HMF selectivity. One possible explanation of this observation was that on clean, highly acidic surfaces, the formed HMF strongly adsorbed onto the surface, resulting in a rapid reduction of accessible strong acid sites on the catalyst surface. In turn, the reduction in accessible strong acid sites led to the rapid reduction in the fructose conversion. Since the surface became sufficiently covered with fructose and fructose breakdown products (e.g., levulinic acid, formic acid, and humins), it is plausible that the residual acidity from these organic acids was responsible for the

residual low level production of HMF, despite the catalyst containing only minimal amounts of accessible strong acid sites (Figure 2B).

To test whether a different catalyst would perform better than the polymeric resin, a mesoporous sulfated zirconia was synthesized using the procedure previously described.[22] The acidity of this material was determined (via titration) to contain 0.36 mmol/g strong acid sites, which was consistent with reported values. Unfortunately, the sulfated zirconia surface was as susceptible to fouling Amberlyst 45, with nearly the same rate of deactivation (Figure 2A). Additionally, under these conditions, the selectivity towards HMF was much lower than with Amberlyst 45, which may reflect the distribution of acid-base sites typical of sulfated zirconia.

3.2.2 Reactions in DMSO

From the perspective of reaction engineering, the substitution of water with polar aprotic solvents is advantageous for several reasons. Most importantly, as the water content is reduced, the reaction kinetics are accelerated in a non-linear manner along with dramatic improvement in HMF selectivity, with yields in excess of 90% commonly reported.[6, 30] Previous work has shown that fructose dehydration follows a specific acid-catalyzed mechanism that has an inverse kinetic isotope effect when comparing reactions in 5% D_2O vs 5% H_2O. This mechanism depends on the [H_3O^+] and is therefore highly influenced by the water content of the solvent. Using thin-film HR-MAS NMR, a previous work reported direct observation of increased [H_3O^+] character with decreasing water content and showed that the acidic protons are localized predominantly within 2 nm of the surface.[31] The kinetic and selectivity effects between fructose dehydration in water and polar aprotic solvents have been well characterized. Although no direct comparison of the solvent effect on deactivation from fouling has been performed, it is a central factor to consider when deciding whether homogeneous or heterogeneous acid catalysts are most suitable for a particular system.

A direct comparison of deactivation and selectivity (see open circles in Figure 2) demonstrates that the use of DMSO led to far slower deactivation, along with much higher selectivity. Given the dramatic effect on the reaction rate and the more labile nature of DMSO compared to water, the reaction conditions needed to be modified in order to minimize DMSO breakdown while achieving similar initial fructose conversions. For 1 M fructose in DMSO, 85% conversion was achieved at a temperature of 120 °C and flow rate of 0.05 ml/min, which was comparable to the conversion rates in water at 0.20 ml/min and 160 °C. As expected, much higher HMF selectivity (80%) was observed with high fructose conversion (>80%) when the reaction was run in DMSO.

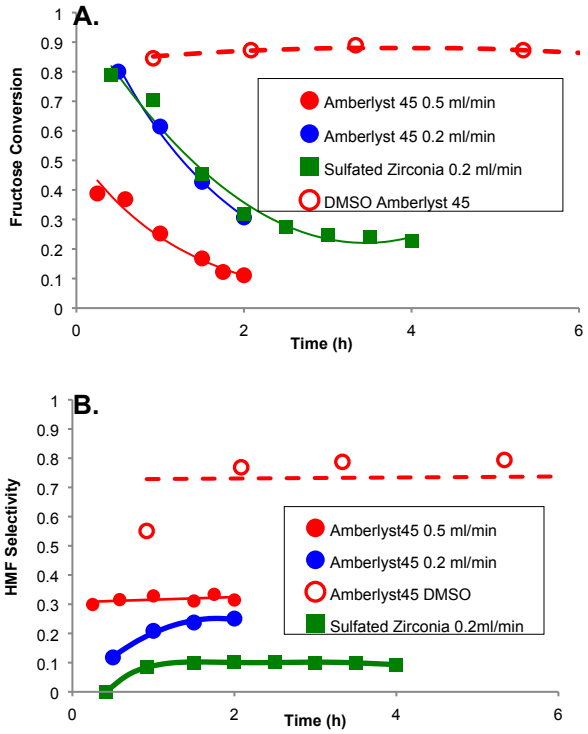

Figure 2. (A) Conversion and (B) HMF selectivity for 1 M fructose run in PFR with water at 160 °C (solid symbols) and DMSO at 120 °C (open symbols).

To provide a normalized comparison of the deactivation rates of 1 M fructose in DMSO and water, Figure 3 gives the conversion as a function of moles fructose/moles SO_3H, which accounts for the different flow rates. The normalized deactivation rates showed that deactivation was five times slower in DMSO than in water. Essentially, this comparison demonstrates that the deactivation in water occurred in nearly stoichiometric ratios so that fouling was the primary issue in terms of improving catalyst stability. Moreover, substitution of DMSO for water as the solvent was not sufficient to eliminate catalyst fouling with a 1 M fructose feed.

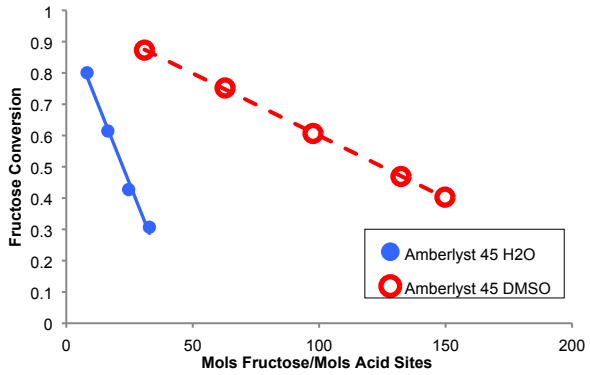

Figure 3. Comparison of catalyst deactivation in H_2O (blue circles) and DMSO (red open circles) normalized to the moles of reactant passed over catalyst bed to the moles of active sites.

3.2.3 Fructose concentration and deactivation rate

Since the deactivation rate was reduced when the flow rate was increased, a series of experiments were carried out to determine the influence of fructose concentration on the deactivation rate. These experiments were performed to determine whether sufficiently reduced fructose concentration in polar aprotic solvents would lead to stable activity on the time scale of days. Results comparing 1 M and 50 mM fructose reactions in DMSO using the same conditions described previously are shown in Figure 4A. Interestingly, virtually no loss in catalyst activity was observed after 70 h on stream when the fructose concentration was reduced 20-fold from 1 M to 50 mM. This result demonstrated that polar aprotic solvents with dilute fructose feeds can dramatically reduce fouling rates and achieve stable reactor operation for extended periods of time. On the other hand, when water was used as the solvent, no significant reduction in the rate of fouling was observed. Comparing the deactivation rates as a function of fructose concentrations (in water) showed a strong linear trend (R^2=0.99, Figure 4B). However, even when the fructose feed concentration was reduced tenfold, the observed deactivation rate of 0.042 h^{-1} was still more then an order of magnitude greater than the rate from sulfur active site breakdown under much more severe hydrothermal conditions.

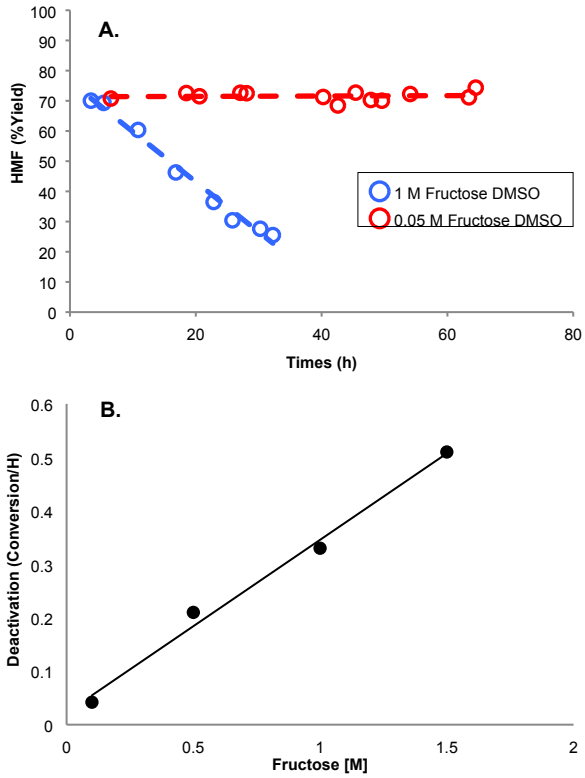

Figure 4. Comparison of the HMF yield obtained using fructose concentrations of 1 M (open blue circles) and 0.05 M (open red circles) in DMSO at 120 °C with a flow rate of 0.05 ml/min (A). The relationship between the deactivation rate and the fructose concentration is shown in (B) for fructose concentrations of 0.1, 0.5, 1.0 and 1.5 M in H_2O reacted at 160 °C with a flow rate of 0.2 ml/min.

3.3 Post-mortem characterization of spent catalyst

Post-mortem characterization of deposited materials on spent catalysts can yield valuable insights into the underlying deactivation mechanisms that originate from the formation of surface residues.[32-34] Solid-state NMR can provide a comprehensive description of the organic deposits found on these material surfaces. Unlike either vibrational or XPS spectroscopy, NMR peak intensities do not depend on transitional matrix elements and are inherently quantitative in nature.[35,36] Additionally ^{13}C NMR spectra have excellent resolution over a broad range when compared to XPS spectroscopy, which requires peak-fitting algorithms to deconvolute overlapping peaks. The principal limitation when using ^{13}C NMR to characterize deposited residues on a catalyst post-mortem is the limited signal-to-noise ratio resulting from a relatively low percentage of ^{13}C nuclei in the catalyst material. The most

common approach to improving the signal is through ^{13}C enrichment, as the natural isotopic abundance of ^{13}C is only 1%. However, the cost for gram scale quantities of ^{13}C enriched materials required is often prohibitive.

An alternative to isotope enrichment is hyperpolarization. In particular, dynamic nuclear polarization (DNP)[37, 38] has been proven a highly effective technique for characterizing surface species in an approach termed DNP surface-enhanced NMR spectroscopy (DNP SENS).[39, 40] DNP relies on a microwave-induced transfer of magnetization from unpaired electrons (introduced as bi-radical polarizing agents) to nuclear spins.[41, 42] In practice, ^{13}C hyperpolarization is achieved by first hyperpolarizing the ^{1}H nuclei and subsequently transferring this magnetization to ^{13}C or other spins using CPMAS or similar methods. DNP SENS can routinely achieve signal to noise improvements that surpass two orders of magnitude, thus, often providing a sensitivity superior to 100% isotope enrichment for ^{13}C.

In addition to obtaining sufficient signal-to-noise ratio, the second hurdle concerns the considerable ^{13}C background signal from the Amberlyst 45 polymer. To circumvent this issue entirely, an analogous set of experiments were run using a commercially available propyl-SO_3H-functionalized porous silica (Silicycle). Given the low intrinsic hydrothermal stability of silica materials, these experiments were run using less severe conditions to limit the breakdown of the silica material itself. To verify that deactivation from deposition was occurring in an analogous fashion on silicycle as with Amberlyst 45, reactions comparing conversion of 50 mM fructose in DMSO and H_2O at 125 °C (normalized to the moles of fructose/moles SO_3H sites) were performed; the results are shown in Figure 5. Under these conditions, deactivation was extremely rapid, with no fructose conversion observed after only 8 moles of fructose per mole of SO_3H had passed over the catalyst. Worth noting is that the catalyst was much more stable when DMSO was the solvent, although, unlike with Amberlyst 45, slow deactivation did occur (0.0051 h^{-1}); this suggested that surface polarity may play an important role in the carbon deposition and warrants further study.

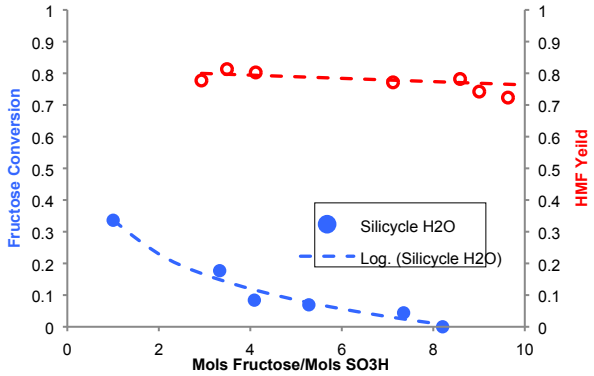

Figure 5: The fructose conversion ratio is plotted as a function of the ratio of fructose to sulfonic acid moieties for dehydration reactions using propyl sulfonic acid functionalized silica "silicycle" in H_2O (blue circles) and DMSO (red circles).

The DNP-enhanced 1D ^{13}C CPMAS and 2D $^{13}C\{^{1}H\}$ PRESTO-HETCOR spectra of the fully deactivated silica material (approximately 48 h TOS) resulting from the reaction of 50 mM fructose in H_2O are shown in Figure 6. Also shown is the reference HR-MAS spectrum of neat U-^{13}C enriched fructose impregnated on the silicycle surface. The spectral assignments are summarized in Table 1. Aside from the peaks attributed to surface-bound O-Si-CH_2-CH_2-CH_2SO_3H groups, the spectra strongly resembled those of native fructose and, to a lesser extent, fructose dehydration products including furans and furan breakdown products (Table 1). We should note that the CH_2 groups in propyl-SO_3H are expected to be represented to a greater extent in the CPMAS spectrum than the quaternary groups of the furanic species or sugar species. Nevertheless, the observed spectra clearly revealed the prominence of propyl-SO_3H groups. This finding was significant as it provided a confirmation that these moieties remained largely intact on the catalyst surface and that hydrolysis of sulfonic acid groups the was not the primary cause of the observed deactivation.

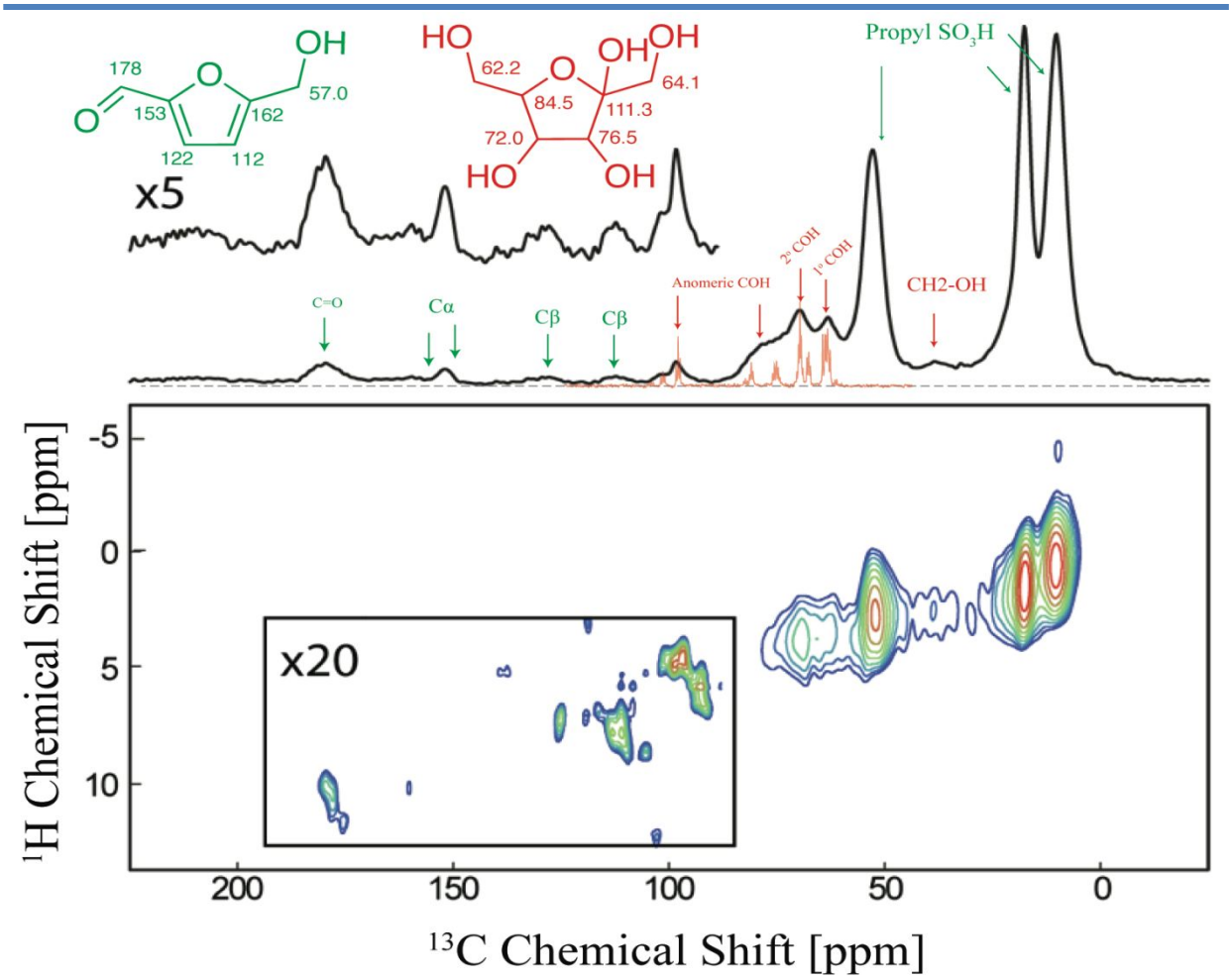

Figure 6: DNP-enhanced ^{13}C CPMAS NMR spectrum of a propyl-SO_3H-silica catalyst with adsorbed carbonaceous residue resulting from the reaction of 50 mM fructose in water at 125 °C for 72 h (top). The HR-MAS ^{13}C NMR spectrum of neat U-^{13}C-enriched fructose that has been impregnated on the silicycle surface is shown below the DNP-enhanced ^{13}C CPMAS NMR spectrum (red trace). The molecular structures of HMF and fructose are shown, and their expected ^{13}C chemical shifts are indicated. The $^{13}C\{^1H\}$ PRESTO-HETCOR spectrum is shown on the bottom. This spectrum only displays correlations between protonated carbon atoms and their attached protons. The assignment of the NMR signals was confirmed by considering the ^{13}C and ^1H isotropic chemical shifts.

Table 1: Assignment of ^{13}C DNP-SENS NMR

Integration limits (ppm)	Assignment
225-200	Ketone
195-172	Aldehyde/COO
171-157	Cα-Furan
156-146	Cα-Furan
143-123	Cβ-Furan
121-107	Cβ-Furan
105-90	*C2-Fructose*
88-74	*C5-Fructose*
74-67	*C3/C4-Fructose*
67-60	*C1/C5-Fructose*
59-45	CH_2SO_3H
44-33	CH_2
25-14	PropylSO_3H
14-5.5	PropylSO_3H

3.4 In situ thin-film HR-MAS NMR spectroscopy

Experimental results from the flow reactor experiments revealed that catalyst deactivation resulted from the deposition of material onto the catalyst surface. Deactivation was accelerated when water was used and slowed with DMSO. Characterization of the residues on the catalyst post-mortem using DNP-enhanced ^{13}C solid-state NMR showed that at moderate temperatures (125 °C), aside from propyl-SO_3H groups, a large fraction of the material resonated at a frequency characteristic of C_{alk}-O-R groups, suggesting that the materials on the surface consisted predominantly of polymerized, partially dehydrated fructose along with a fraction of furanics and other breakdown products of HMF.

One critical question that remained ambiguous, with only post-mortem data, was the nature of the initial deposits on the catalyst surface. One plausible deposition pathway involves fructose initially undergoing dehydration to form furans, followed by the furans being absorbed onto the catalyst surface, and finally these furans serving as seeds for the subsequent addition of fructose molecules to form a carbonaceous layer that blocks the acid sites. Alternatively, one could imagine that, prior to undergoing dehydration, fructose adsorbs onto the surface and undergoes polymerization with some fraction of the polymer undergoing dehydration to form a furanic component. A third possible explanation is that both furanics and fructose exhibit a high affinity for the catalyst surface and simultaneously deposit to form the carbonaceous layer. To distinguish between these different scenarios, In situ ^{13}C NMR with thin liquid layers impregnated onto the catalyst surface was used to obtain a real-time picture of the solid-liquid interface.[5, 31, 43, 44]

Molecular behavior at solid-liquid interfaces can be probed using solid-state NMR of solid materials impregnated with liquid films (1-4 nm liquid thickness). In situ HR-MAS NMR is ideally suited to study solid-liquid interfaces, as these systems exhibit molecular dynamics intermediate to those of isotropic liquids and rigid solids, allowing for high resolution spectra under moderate MAS frequency. This approach has been adapted for measuring the ^{13}C NMR spectra of U-^{13}C-enriched fructose dissolved in D_2O and d_6-DMSO and impregnated onto a propyl-SO_3H-functionalized silica. Given the minimal precedent in the literature, we investigated the interfacial behavior of the liquid impregnated into the porous solid by comparing spectra acquired under static and MAS conditions. ^{1}H and ^{13}C NMR spectra acquired under static and 25 kHz MAS are compared in Figure 7. There was a dramatic improvement in spectral resolution under MAS. For example, ^{13}C-^{13}C *J* couplings could be readily resolved in the ^{13}C NMR spectra and many peaks in the ^{1}H NMR spectra had nearly solution-like line width (ca. 20 Hz FWHM). The substantial improvement in resolution under application of MAS suggested that the solvent and fructose molecules within the thin liquid layer had hindered rotation and diffusion. In order for MAS to yield improved resolution, the correlation time of the molecules should typically be longer than the rotor period (inverse of the MAS frequency).[45, 46] MAS will also help to narrow the lines by averaging susceptibility and magnetic field inhomogeneity over the sample.

Considering the dramatic effects of the solvent on the reaction rates and selectivity, the manner in which the solvent influenced the HR-MAS ^{13}C and ^{1}H NMR spectra of fructose was investigated by impregnating idealized 2 nm layers of 1 M fructose in either d_6-DMSO or D_2O (0.66uL/mg) onto propyl-SO_3H-functionalized silica. The measurements were conducted prior to the fructose undergoing any significant reaction. The ^{13}C (Figure 8A) and ^{1}H (Figure 8B) NMR spectra obtained with D_2O and d_6-DMSO showed distinct differences. First, a comparison of ^{13}C NMR spectra showed that fructose in d_6-DMSO contained several peaks that were partially shifted to higher frequency along with broadening at the C2 (103 ppm) C3 (76 ppm) and C4 (82 ppm) positions. This shift of the C-OH carbons to a higher chemical shift in d_6-DMSO suggested a greater degree of protonation of hydroxyls resulting

from increased [H_3O^+] due to the lower water concentration. This difference was more obvious when comparing ^{1}H spectra (Figure 8B), which show that the major peak comprising the C-OH-H_2O-H_3O^+ hydrogen bonded network shifted by almost 1 ppm in d_6-DMSO, when compared to D_2O. An additional surprise was that in d_6-DMSO, some HMF had begun to form without any external heat being applied beyond the frictional heating from 25 kHz MAS (ca. +30°C).

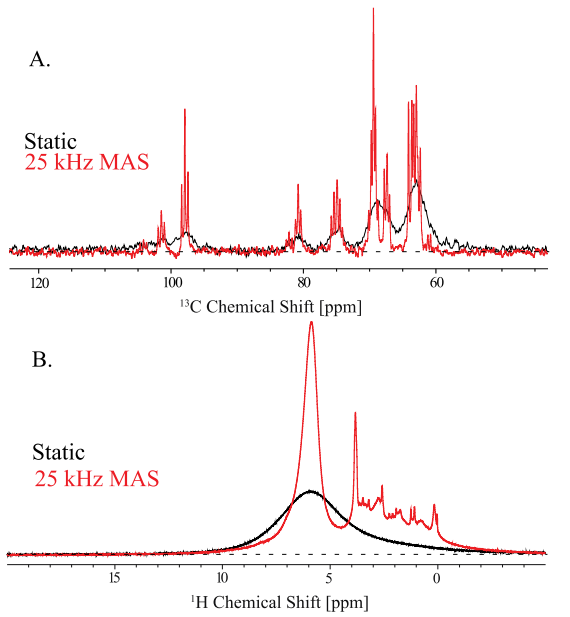

Figure 7: HR-MAS ^{13}C (A) and ^{1}H (B) NMR of uniformly ^{13}C enriched fructose (98%) in DMSO impregnated with an idealized 2 nm liquid layer (0.66µl/mg) onto propyl-SO_3H-functionalized silica gel. Comparison of the static (black line) vs. MAS with 25 kHz frequency (red line) are shown for ^{13}C (A) and ^{1}H (B).

In situ measurements were made by heating the stator to 50 °C, which, along with the ca. 30 °C temperature increase from frictional heating, raised the sample temperature to ca. 80 °C (Figure 9). As expected, the samples in DMSO reacted much more rapidly than in D_2O, and showed significant formation of HMF after a relatively brief period (e.g. < 1 h). Recognizing that the primary goal of these measurements was to probe the sequence in which materials were being deposited onto the catalyst surface, NMR was used to directly compare the relative molecular mobility of different species. This was accomplished by comparing ^{13}C NMR spectra measured via direct polarization (herein referred to simply as MAS) and ^{1}H–^{13}C cross-polarization (CPMAS). The CP transfers are primarily mediated through ^{1}H-^{13}C heteronuclear dipolar couplings, which are motionally averaged to zero for molecules that were undergoing rapid isotropic motions. Therefore, the CPMAS spectra primarily showed NMR signals from immobilized molecules or molecules with restricted rotation. On the other hand, the MAS NMR spectra were expected to show NMR signals from both mobile and immobile molecules, although the former should give rise to sharper NMR signals and be over-represented in the MAS NMR spectrum.

Prior to the reaction of fructose, no ^{13}C CPMAS NMR signal was observed for fructose in either d_6-DMSO or D_2O. However, following several hours of reaction, clear differences were observed in NMR spectra obtained from the d_6-DMSO and D_2O samples. As expected, HMF was formed much more rapidly in DMSO, and with nearly 100% selectivity. Furthermore, the HMF formed in DMSO was highly mobile, as evidenced by the lack of any detectable CPMAS ^{13}C NMR signal, even with a long CP contact time of 8 ms (Figure 9A).The sample with D_2O showed very different behavior. After allowing the D_2O sample to react overnight, a significant CPMAS ^{13}C NMR signal was observed with a CP contact time of only 3 ms. This strongly suggested that a significant fraction of the product molecules in D_2O was immobilized on the silica surface. The comparable intensity of the CPMAS and MAS ^{13}C NMR signals of the dehydration products and fructose suggested that the deposition was initiated by the adsorption of the dehydrated products onto the catalyst surface, which was then followed by additional polymerization with fructose molecules to form a carbonaceous layer.

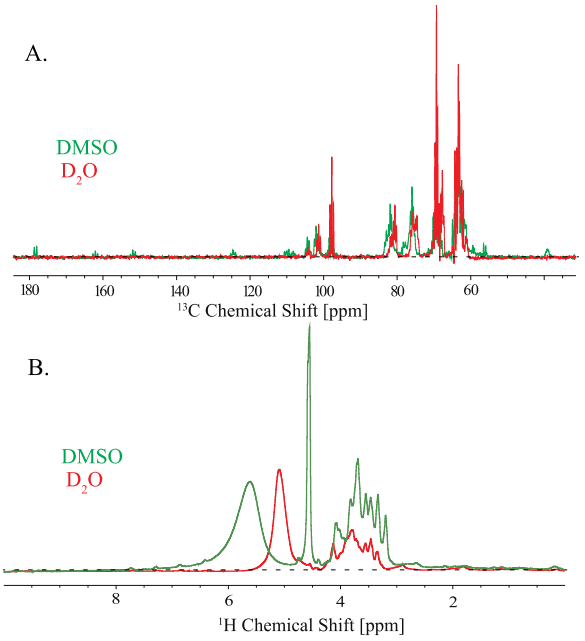

Figure 8: Comparison of the solvent effect with HR-MAS NMR of uniformly ^{13}C-enriched fructose (98%) impregnated with an idealized 2 nm liquid layer (0.66µl/mg) onto propyl-SO_3H functionalized silica gel. Shown in (A) and (B) are ^{13}C and ^{1}H NMR spectra, respectively, taken with D_2O (red) and DMSO (green) as solvents.

Finally, the effect of the solvent on the molecular mobility of purified HMF on the surface, prior to any reaction, was studied using ^{1}H HR-MAS NOESY experiment. Due to hindered motion of the molecules at the catalyst surface the primary source of the cross-peaks is from zero-quantum ^{1}H spin diffusion. This process is accelerated when the mobility is reduced and as such less mobile species should feature a faster build-up of cross-peaks. The catalysts were impregnated with 1M HMF (natural abundance ^{13}C) in D_2O or d_6-DMSO. 2D ^{1}H NOESY NMR spectra were acquired with spin diffusion mixing times τ_{mix} = 40 ms or 320 ms (Figure 10). We note that due to the preponderance of HMF on the surface, the spectra are dominated by resonances H1-H4 attributed to HMF (see the inset in Figure 10). In addition, the acidic ^{1}H in propyl-SO_3H groups are most likely exchanged with deuterium. Importantly, only the spectra taken in D_2O show the intramolecular ^{1}H-^{1}H correlations within the HMF molecule (represented by red lines in Figure 10). Specifically, in the D_2O-impregnated sample, H2-H3 and H3-H4 correlation signals were observed in the 2D ^{1}H NOESY spectrum with τ_{mix} = 40 ms. When τ_{mix} was extended to 320 ms, additional correlation signals (H1-H2, H1-H3, H1-H4, and H2-H4) appeared. In contrast, none of these correlations were detected in the 2D ^{1}H NOESY spectra of the DMSO-impregnated sample, which suggests that HMF molecules are less mobile and interact far more strongly with the catalyst surface in D_2O than in d_6-DMSO. This result is consistent with the other experimental data showing much stronger affinity for molecules to adsorb on the surface and rapid formation of a carbonaceous layer when water was used as the solvent.

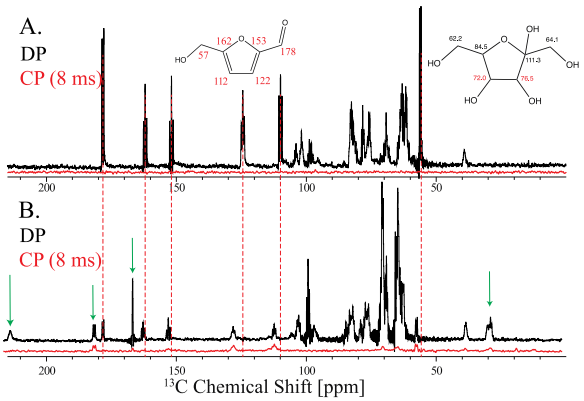

Figure 9: In situ HR-MAS ^{13}C NMR of fructose impregnated onto propyl-SO_3H-functionalized silica gel. Comparison of CPMAS (red) and MAS (black) spectra of samples including a 2 nm thick layer of DMSO (A) and D_2O (B). The fructose concentration was 2 M. The NMR spectra are shown after reaction for 12 hours at 80 °C. Dashed red lines highlight the peak positions from HMF and show that HMF is principally formed in DMSO. Green arrows indicate the HMF breakdown products formic and levulinic acid.

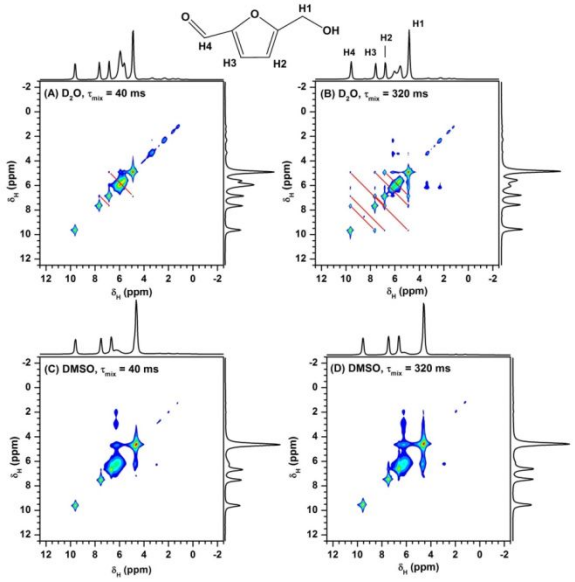

Figure 10: HR-MAS NOESY ^{1}H NMR of HMF impregnated onto propyl-SO_3H-functionalized silica gel. (A) D_2O, τ_{mix} = 40 ms; (B) D_2O, τ_{mix} = 320 ms; (C) DMSO τ_{mix} = 40 ms; and (D) DMSO, τ_{mix} = 320 ms.

4. Conclusions

To comprehensively investigate solid acid hydrothermal stability, a number of commercially available sulfonated materials were surveyed, including state-of-the-art resins under conditions without any reactant present. As expected, nearly all of these materials showed very poor stability, except for Amberlyst 45 (a halogenated cross-linked resin), which was significantly more resistant to hydrothermal breakdown of the sulfonic acid sites. Deactivation, however, occurred two orders of magnitude faster when a reactant was introduced to the reactor. The results clearly demonstrated that the dominant mode of catalyst deactivation for these reactions run under aqueous conditions is from fouling, and that fouling should therefore be an integral consideration in efforts to improve the hydrothermal stability of solid acid catalysts used in the conversion of oxygenated molecules.

Additionally, it was demonstrated that one viable route to overcoming catalyst fouling was the use of use polar aprotic solvents with dilute feed streams. Moreover, when comparing the stability of different solid acid catalysts, choice of support materials was found to play a significant role, with polymeric materials displaying excellent stability, while functionalized silicas deactivated relatively rapidly.

For solid acid catalysts to be industrially useful for dehydration of polyhydric alcohols in water, the catalyst will either require methods to regenerate the catalyst or methods to prevent humin formation altogether. A route demonstrated here to accomplish this is through engineering the support material along with the solvent system to allow for reactants and products to easily desorb from the surface.

▪ AUTHOR INFORMATION

bshanks@iastate.edu

▪ ACKNOWLEDGEMENTS

The authors would like to acknowledge NSF Award number EEC-0813570 for generously supporting this work. At Ames Laboratory, this research was supported by the U.S. DOE, Office of Science, Office of BES, Division of Chemical Sciences, Geosciences, and Biosciences. Ames Laboratory is operated for the DOE by Iowa State University under Contract No. DE-AC02- 07CH11358.

▪ REFERENCES

(1) Gilkey, M.J.; Mironenko, A.V.; Vlachos, D.G.; Xu, B. Adipic acid production via metal-free selective hydrogenolysis of biomass-derived tetrahydrofuran-2, 5-dicarboxylic acid. *ACS Catal.* **2017**, 7, 6619-6634.

(2) Xie, J.; Duan, P.; Kaylor, N.; Yin, K.; Huang, B.; Schmidt-Rohr, K.; Davis, R.J. Deactivation of Supported Pt Catalysts during Alcohol Oxidation Elucidated by Spectroscopic and Kinetic Analyses. *ACS Catal.* **2017**, 7, 6745-6756.

(3) Lopez-Ruiz, J.A.; Cooper, A.R.; Li, G.; Albrecht, K.O. Enhanced Hydrothermal Stability and Catalytic Activity of $La_xZr_yO_z$ Mixed Oxides for the Ketonization of Acetic Acid in the Aqueous Condensed Phase. *ACS Catal.* **2017**, 7, 6400-6412.

(4) Donoeva, B.; Masoud, N.; de Jongh, P.E. Carbon Support Surface Effects in the Gold-Catalyzed Oxidation of 5-Hydroxymethylfurfural. *ACS Catal.* **2017**, 7, 4581-4591.

(5) Qi, L.; Alamillo, R.; Elliott, W.A.; Andersen, A.; Hoyt, D.W.; Walter, E.D.; Han, K.S.; Washton, N.M.; Rioux, R.M.; Dumesic, J.A.; Scott, S.L. Operando Solid-State NMR Observation of Solvent-Mediated Adsorption-Reaction of Carbohydrates in Zeolites. *ACS Catal.* **2017**, 7, 3489-3500.

(6) Mellmer, M.A.; Sener, C.; Gallo, J.M.R.; Luterbacher, J.S.; Alonso, D.M.; Dumesic, J.A. Solvent effects in acid-catalyzed biomass conversion reactions. *Angew. Chem. Int. Ed.* **2014**, 53, 11872-11875.

(7) Seemala, B.; Cai, C.M.; Wyman, C.E.; Christopher, P. Support Induced Control of Surface Composition in Cu–Ni/TiO_2 Catalysts Enables High Yield Co-Conversion of HMF and Furfural to Methylated Furans. *ACS Catal.* **2017**, 7, 4070-4082.

(8) Tucker, M.H.; Crisci, A.J.; Wigington, B.N.; Phadke, N.; Alamillo, R.; Zhang, J.; Scott, S.L.; Dumesic, J.A. Acid-Functionalized SBA-15-Type Periodic Mesoporous Organosilicas and Their Use in the Continuous Production of 5-Hydroxymethylfurfural. *ACS Catal.* **2012**, 2, 1865-1876.

(9) Nguyen, H.; Xiao, N.; Daniels, S.; Marcella, N.; Timoshenko, J.; Frenkel, A.; Vlachos, D.G. Role of Lewis and Brønsted Acidity in Metal Chloride Catalysis in Organic Media: Reductive Etherification of Furanics. *ACS Catal.* **2017**, 7, 7363-7370.

(10)Brown, R.C., *Biorenewable Resources: Engineering New Products from Agriculture*. 2003: Blackwell Publishing.

(11) Akbar, J.; Massey, S. Kinetics and mechanism of thermal degradation of pentose- and hexose-based carbohydrate polymers. R. *Carbohydrate Polym.* **2012**, 90, 1386-1393.
(12) Yaylayan, V.A.; Keyhani, A. Carbohydrate and Amino Acid Degradation Pathways in l-Methionine/d-[^{13}C] Glucose Model Systems. *J. Agric. Food Chem.* **2001**, 49, 800-803.
(13) Adams, A.; Tehrani, K.A.; Kersiene, M.; Venskutonis, R.; De, K.N. Characterization of Model Melanoidins by the Thermal Degradation Profile. *J. Agric. Food Chem.* **2003**, 51, 4338-4343.
(14) Pham, H.N.; Anderson, A.E.; Johnson, R.L.; Schwartz, T.J.; O'Neill, B.J.; Duan, P.; Schmidt-Rohr, K.; Dumesic, J.A.; Datye, A.K. Carbon Overcoating of Supported Metal Catalysts for Improved Hydrothermal Stability. *ACS Catal.* **2015**, 5, 4546-4555.
(15) Jongerius, A.L.; Copeland, J.R.; Foo, G.S.; Hofmann, J.P.; Bruijnincx, P.C.A.; Sievers, C.; Weckhuysen, B.M. Stability of Pt/γ-Al_2O_3 Catalysts in Lignin and Lignin Model Compound Solutions under Liquid Phase Reforming Reaction Conditions. *ACS Catal.* **2013**, 3, 464-473.
(16) Ravenelle, R.M.; Copeland, J.R.; Kim, W.-G.; Crittenden, J.C.; Sievers, C. Structural Changes of γ-Al_2O_3-Supported Catalysts in Hot Liquid Water. *ACS Catal.* **2011**, 1, 552-561.
(17) Nielsen, M.; Brogaard, R.Y.; Falsig, H.; Beato, P.; Swang, O.; Svelle, S. Kinetics of Zeolite Dealumination: Insights from H-SSZ-13. *ACS Catal.* **2015**, 5, 7131-7139.
(18) Gardner, D.W.; Huo, J.; Hoff, T.C.; Johnson, R.L.; Shanks, B.H.; Tessonnier, J.-P. Insights into the Hydrothermal Stability of ZSM-5 under Relevant Biomass Conversion Reaction Conditions. *ACS Catal.* **2015**, 5, 4418-4422.
(19) Anderson, J.M.; Johnson, R.L.; Schmidt-Rohr, K.; Shanks, B.H. Chemical Structure and Hydrothermal Deactivation of Moderate-Temperature Carbon Materials with Acidic SO_3H Sites. *Carbon* **2014**, 74, 333-345.
(20) Long, W.; Jones, C.W. Hybrid Sulfonic Acid Catalysts Based on Silica-Supported Poly(Styrene Sulfonic Acid) Brush Materials and Their Application in Ester Hydrolysis. *ACS Catal.* **2011**, 1, 674-681.
(21) Siril, P.F.; Cross, H.E.; Brown, D.R. New polystyrene sulfonic acid resin catalysts with enhanced acidic and catalytic properties. *J. Mol. Catal. A: Chem.* **2008**, 279, 63-68.
(22) Osatiashtiani, A.; Lee, A.F.; Granollers, M.; Brown, D.R.; Olivi, L.; Morales, G.; Melero, J.A.; Wilson, K. Hydrothermally Stable, Conformal, Sulfated Zirconia Monolayer Catalysts for Glucose Conversion to 5-HMF. *ACS Catal.* **2015**, 5, 4345-4352.
(23) Ide, M.S.; Falcone, D.D.; Davis, R.J. On the deactivation of supported platinum catalysts for selective oxidation of alcohols. *J. Catal.* **2014**, 311, 295-305.
(24) Morales, G.; Osatiashtiani, A.; Hernandez, B.; Iglesias, J.; Melero, J.A.; Paniagua, M.; Brown, D.R.; Granollers, M.; Lee, A.F.; Wilson, K. Conformal sulfated zirconia monolayer catalysts for the one-pot synthesis of ethyl levulinate from glucose. *Chem. Commun.* **2014**, 50, 11742-11745.
(25) Sauvée, C.; Rosay, M.; Casano, G.; Aussenac, F.; Weber, R.T.; Ouari, O.; Tordo, P. Highly efficient, water-soluble polarizing agents for dynamic nuclear polarization at high frequency. *Angew. Chem. Int. Ed.* **2013**, 52, 10858-10861.
(26) Zhao, X.; Hoffbauer, W.; Schmedt auf der Günne, J.; Levitt, M.H. Heteronuclear polarization transfer by symmetry-based recoupling sequences in solid-state NMR. *Solid State Nucl. Magn. Reson.* **2004**, 26, 57-64.
(27) Sardo, M.; Siegel, R.; Santos, S.M.; Rocha, J.; Gomes, J.R.B.; Mafra, L. Combining multinuclear high-resolution solid-state MAS NMR and computational methods for resonance assignment of glutathione tripeptide. *J. Phys. Chem. A* **2012**, 116, 6711-6719.
(28) Bielecki, A.; Kolbert, A.C.; Levitt, M.H. Frequency-switched pulse sequences: Homonuclear decoupling and dilute spin NMR in solids. *Chem. Phys. Lett.* **1989**, 155, 341-346.
(29) Nolan, M.R.; Sun, G.; Shanks, B.H. On the selective acid-catalysed dehydration of 1,2,6-hexanetriol. *Catal. Sci. Tech.* **2014**, 4, 2260-2266.
(30) Zhang, J.; Das, A.; Assary, R.S.; Curtiss, L.A.; Weitz, E. A combined experimental and computational study of the mechanism of fructose dehydration to 5-hydroxymethylfurfural in dimethylsulfoxide using Amberlyst 70, PO_4^{3-}/niobic acid, or sulfuric acid catalysts. *Appl. Catal. B: Environ.* **2016**, 181, 874-887.
(31) Johnson, R.L.; Hanrahan, M.P.; Mellmer, M.; Dumesic, J.A.; Rossini, A.J.; Shanks, B.H. Solvent-Solid Interface of Acid Catalysts Studied by High Resolution MAS NMR. *J. Phys. Chem. C* **2017**, 121, 17226-17234.
(32) Schwartz, T.J.; Johnson, R.L.; Cardenas, J.; Okerlund, A.; Da Silva, N.A.; Schmidt-Rohr, K.; Dumesic, J.A. Engineering catalyst microenvironments for metal-catalyzed hydrogenation of biologically derived platform chemicals. *Angew. Chem. Int. Ed.* **2014**, 53, 12718-12722.

(33) Johnson, R.L.; Perras, F.A.; Kobayashi, T.; Schwartz, T.J.; Dumesic, J.A.; Shanks, B.H.; Pruski, M. Identifying Low-Coverage Surface Species on Noble Metal Nanoparticles by DNP-NMR. *Chem. Commun.* **2016**, 52, 1859-1862.

(34) Perras, F.A.; Padmos, J.D.; Johnson, R.L.; Wang, L.-L.; Schwartz, T.J.; Kobayashi, T.; Horton, J.H.; Dumesic, J.A.; Shanks, B.H.; Johnson, D.D.; Pruski, M. Characterizing Substrate-Surface Interactions on Alumina-Supported Metal Catalysts by DNP-Enhanced Double-Resonance NMR Spectroscopy. *J. Amer. Chem. Soc.* **2017**, 139, 2702-2709.

(35) Johnson, R.L.; Schmidt-Rohr, K. Quantitative solid-state ^{13}C NMR with signal enhancement by multiple cross polarization. *J. Magn. Reson.* **2014**, 239, 44-49.

(36) Duan, P.; Schmidt-Rohr, K. Composite-pulse and partially dipolar dephased multiCP for improved quantitative solid-state ^{13}C NMR. *J. Magn. Reson.* **2017**, 285, 68-78.

(37) Maly, T.; Debelouchina, G.T.; Bajaj, V.S.; Hu, K.-N.; Joo, C.-G.; Mak–Jurkauskas, M.L.; Sirigiri, J.R.; van der Wel, P.C.A.; Herzfeld, J.; Temkin, R.J.; Griffin, R.G. Dynamic nuclear polarization at high magnetic fields. *J. Chem. Phys.* **2008**, 128, 052211 (1-19).

(38) Ni, Q.Z.; Daviso, E.; Can, T.V.; Markhasin, E.; Jawla, S.K.; Swager, T.M.; Temkin, R.J.; Herzfeld, J.; Griffin, R.G. High frequency dynamic nuclear polarization. *Acc. Chem. Res.* **2013**, 46, 1933-1941.

(39) Lesage, A.; Lelli, M.; Gajan, D.; Caporini, M.A.; Vitzthum, V.; Miéville, P.; Alauzun, J.; Roussey, A.; Thieuleux, C.; Mehdi, A.; Bodenhausen, G.; Coperet, C.; Emsley, L. Surface Enhanced NMR Spectroscopy by Dynamic Nuclear Polarization. *J. Amer. Chem. Soc.* **2010**, 132, 15459-15461.

(40) Rossini, A.J.; Zagdoun, A.; Lelli, M.; Lesage, A.; Copéret, C.; Emsley, L. Dynamic Nuclear Polarization Surface Enhanced NMR Spectroscopy. *Acc. Chem. Res.* **2013**, 46, 1942-1951.

(41) Song, C.; Hu, K.-N.; Joo, C.-G.; Swager, T.M.; Griffin, R.G. TOTAPOL: A Biradical Polarizing Agent for Dynamic Nuclear Polarization Experiments in Aqueous Media. *J. Amer. Chem. Soc.* **2006**, 128, 11385-11390.

(42) Hu, K.-N.; Yu, H.-h.; Swager, T.M.; Griffin, R.G. Dynamic nuclear polarization with biradicals. *J. Amer. Chem. Soc.* **2004**, 126, 10844-10845.

(43) Chen, K.; Kelsey, J.; White, J.L.; Zhang, L.; Resasco, D. Water Interactions in Zeolite Catalysts and Their Hydrophobically Modified Analogues. *ACS Catal.* **2015**, 5, 7480-7487.

(44) Chen, K.; Damron, J.; Pearson, C.; Resasco, D.; Zhang, L.; White, J.L. Zeolite Catalysis: Water Can Dramatically Increase or Suppress Alkane C–H Bond Activation. *ACS Catal.* **2014**, 4, 3039-3044.

(45) Sarkar, R.; Mainz, A.; Busi, B.; Barbet-Massin, E.; Kranz, M.; Hofmann, T.; Reif, B. Immobilization of soluble protein complexes in MAS solid-state NMR: Sedimentation versus viscosity. *Solid State Nucl. Magn. Reson.* **2016**, 76-77, 7-14.

(46) Mainz, A.; Jehle, S.; van Rossum, B.J.; Oschkinat, H.; Reif, B. Large protein complexes with extreme rotational correlation times investigated in solution by magic-angle-spinning NMR spectroscopy. *J. Amer. Chem. Soc.* **2009**, 131, 15968-15969.

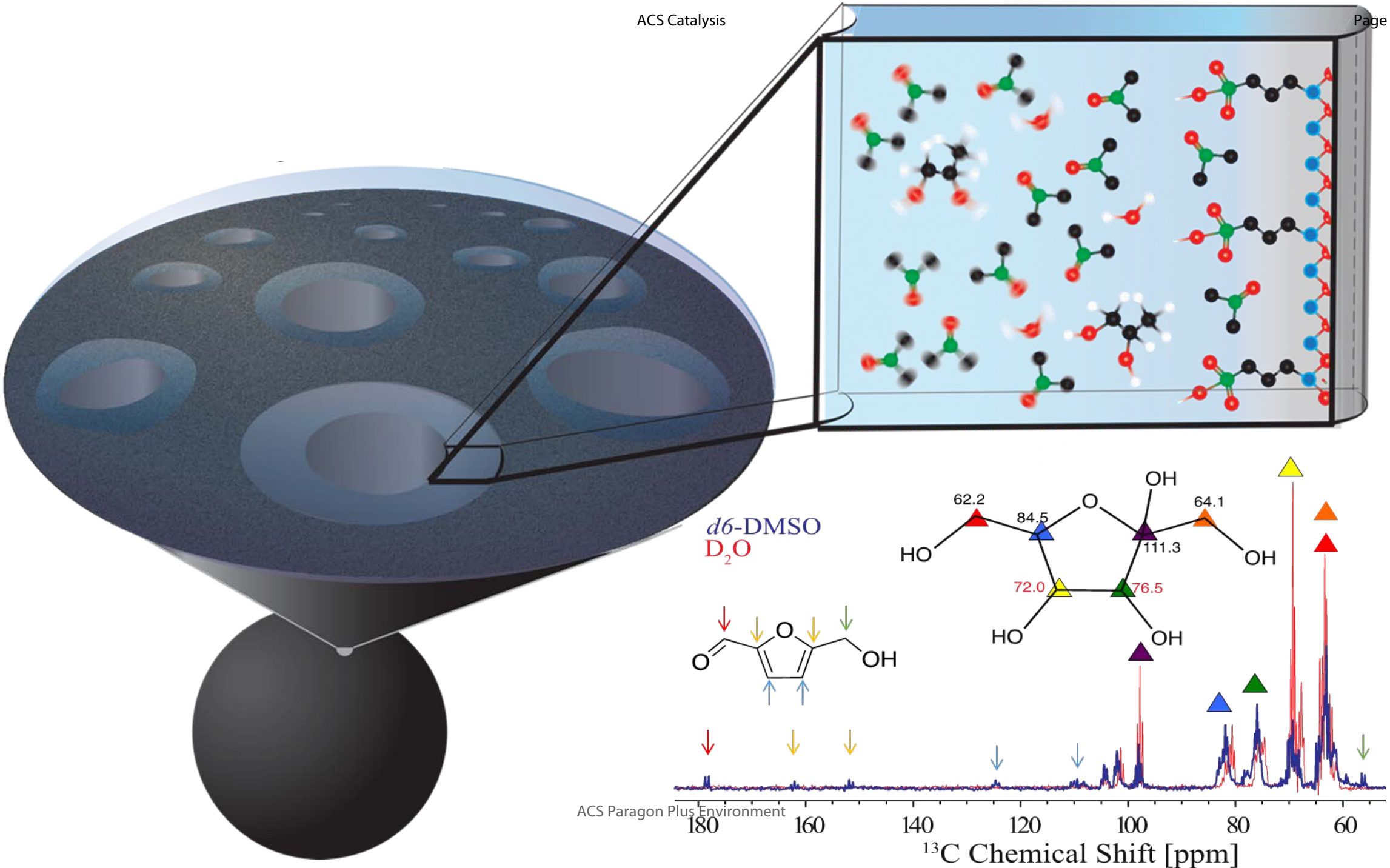
d6-DMSO
D2O
62.2
84.5
64.1
111.3
72.0
76.5
HO
OH
O
180
160
140
120
100
80
60
13C Chemical Shift [ppm]